

## Isomorphous substitution effect on the vibration frequencies of hydroxyl groups in molecular cluster models of the clay octahedral sheet

CLARO I. SAINZ-DIAZ,<sup>1,\*</sup> VICENTE TIMON,<sup>2</sup> VICENTE BOTELLA,<sup>2</sup> AND ALFONSO HERNANDEZ-LAGUNA<sup>1</sup>

<sup>1</sup>Estacion Experimental del Zaidin (C.S.I.C.), C/Profesor Albareda, 1, 18008-Granada, Spain

<sup>2</sup>Instituto de Estructura de la Materia (C.S.I.C.), C/Serrano 113, 28006-Madrid, Spain

### ABSTRACT

The geometrical features and electronic structure of molecular clusters models of two octahedrally coordinated cations in edge-sharing octahedra were studied by means of Hartree-Fock ab initio molecular orbital calculations at LANL2DZ and 6-31+G\* levels. These models represent the different cation pairs among  $\text{Al}^{3+}$ ,  $\text{Fe}^{3+}$ , and  $\text{Mg}^{2+}$  of the octahedral sheet of clays. These models reproduce the experimental values of the main geometrical features in the corresponding minerals. The vibrational frequencies of the bridging hydroxyl groups (M-OH-M') were calculated and compared with experimental data. A good agreement between theoretical and experimental results was found. The relative differences of  $\nu(\text{OH})$  and  $\delta(\text{OH})$  frequencies calculated among these (M-OH-M') cation pairs are similar to the experimental behavior in clays. Theoretical  $\gamma(\text{OH})$  frequencies were also calculated and presented as an estimation of the experimental. Correlations between the atomic weights and the atomic Mulliken charges of the cations with the experimental and theoretical OH vibration frequencies have been also determined and a similar behavior was found.

### INTRODUCTION

Smectites and other related 2:1 phyllosilicate clay minerals share the common structural feature that two tetrahedral layers sandwich a sheet of octahedrally coordinated cations. The great diversity of these silicates occurs because of their capacity for isomorphous substitution of various cations in octahedral and tetrahedral sheets, providing different properties in the interlayer space (Güven 1988). In dioctahedral clays, isomorphous substitution  $\text{Al}^{3+}$  by  $\text{Mg}^{2+}$  in the octahedral sheet, or  $\text{Si}^{4+}$  by  $\text{Al}^{3+}$  in the tetrahedral sheet results in a net negative charge, which is compensated by additional cations in the interlayer space. The valuable catalytic and adsorptive properties of clays motivate theoretical study of their structure and behavior. Such studies can also be useful to understand some mineral transformations and some industrial applications of clays, like catalysis, and nuclear waste and pollutant disposal barrier component.

The interlayer space and cation distribution in the tetrahedral sheet of these minerals were studied previously (Güven 1988; Karaborni et al. 1996 and references therein), but the properties of the octahedral sheet have received scant attention. The cation ordering of the octahedral sheet of these minerals is important in natural transformations and dehydroxylation processes. The cations of this layer are octahedrally coordinated with six anions, at least two of which are hydroxyl groups. Most properties of these OH groups will depend on the nature of the cations joined to them.

Many XRD studies of 2:1 clay structures are reported, but these give no indication of the proton positions within the hydroxyl groups. IR studies of muscovite (Vedder 1964) and electrostatic calculations (Giese 1979) have suggested that the orientation of these hydroxyl groups is sensitive to the struc-

ture of the octahedral sheet. The study of the structure and properties of these hydroxyl groups is interesting, because they can play a major role in the catalytic activity of these minerals, in their interactions with water, other molecules and cations. Additionally, the octahedral cations can play a significant role in sorption and dissolution phenomena in many minerals, where OH groups can have varying effects on the reactivity of mineral surface (Schindler and Stumm 1987).

Spectroscopic methods are especially useful for studying clay structure, because they probe local atomic environments and have the potential to determine indirectly short-range cation ordering. IR data exists for stretching ( $3700\text{--}3500\text{ cm}^{-1}$ ) (Besson and Drits 1997; Madejová et al. 1994) and bending ( $700\text{--}1000\text{ cm}^{-1}$ ) (Cuadros and Altaner 1998) OH vibrations in clays. However, it is difficult to obtain experimentally an accurate identification and quantitative study of the cation distribution in these systems. Hence, computer simulations can play a critical role, such as, Reverse Monte Carlo simulations (Cuadros et al. 1999).

Some modeling of clays have been reported applying empirical interatomic potentials (Collins and Catlow 1992; Bleam 1993). However, clay structures are difficult to treat using empirical forcefield methods. Hydrogen bonding, low symmetry and relatively weak interactions in the interlayer space require at least the more sophisticated and exact methods provided by the molecular orbital theory. To study the chemical-physical properties of solids by means of quantum mechanical theory, two main models can be considered: a semi-infinite model and a local model. The first one studies the mineral crystal in its whole extension, the electrons can be described by plane waves (Payne et al. 1992) or LCAO (Orlando et al. 1994; Sanchez-Portal et al. 1997) approaches and the unit cell is extended by a translation periodicity of the crystal. There are different approaches and applications in this model giving important re-

\*E-mail: sainz@eez.csic.es

sults, specially describing properties related with the whole bulk crystal (crystal structure, equation of state, lattice vibrations, etc.), see reviews of Tossell and Vaughan (1992), Payne et al. (1992), and Sauer et al. (1994). The second model is used cutting a small piece of the solid that includes the main information for studying one chemical-physical property of the mineral. Then, the mineral is modeled by a cluster or molecular model, taking into account the nature of the mineral bonds. This method is considered to be very fruitful to study local properties of the solid. The influence of the cation isomorphous substitution on the vibrational frequencies of the hydroxy groups in the octahedral sheet of clays is a phenomenon depending on a local environment and the choice of a right cluster model can be a good approach for its study. Periodic *ab initio* methods have been used in the study of some mineral structures (Bridgeman et al. 1996; Becker et al. 1996; Sherman 1991; Smrcok and Benco 1996; Winkler et al. 1994, 1995). Hobbs et al. (1997) obtained an all-atom geometry optimization of kaolinite using a periodic *ab initio* method based on DFT with interesting results. Many approximations were reported applying quantum mechanical studies on clusters or molecular models of these infinite structures with interesting results (Lasaga 1992; Sauer 1989; Sauer et al. 1994; Kubicki et al. 1996). Interesting theoretical studies exist of formation of adsorption complexes on the surfaces of minerals and dissolution kinetics by means of molecular cluster in silica (Sauer 1989; Sauer et al. 1994) and aluminosilicates (Lasaga 1992, 1995; Xiao and Lasaga 1994; Kubicki et al. 1996). Organic acid adsorption on aluminosilicates has been studied theoretically with molecular clusters (Kubicki et al. 1997). Recently, *ab initio* studies with molecular clusters of aluminium oxides and oxyhydroxides (Kubicki and Apitz 1998) and aluminium-oxide-carboxylate complexes (Kubicki et al. 1999) have been reported. These studies show that the use of molecular cluster models can be a valid approach for studying some physical-chemical properties of minerals at microscopic scale. This work uses theoretical methods to understand the influence of the isomorphous cation substitution on the structural and vibrational properties of hydroxyl groups in the octahedral sheet of clays.

## MODELS AND METHODOLOGY

Our molecular model is a meaningful structure that includes at least one OH group, two cations of the octahedral sheet and the atoms of the first co-ordination sphere of both cations. The tetrahedral sheet and interlayer cation effect are considered constant in the study of isomorphous substitution effect of cations in the octahedral sheet. Our model contains the most relevant and closer features to study the relative effect of the isomorphous cation substitution in the octahedral sheet on the OH vibration frequencies, as is shown by comparison with the experiment below. Moreover, this model must represent various cation pairs that are common in dioctahedral clays. This model was generated from crystallographic data of pyrophyllite  $[\text{Si}_8\text{Al}_4\text{O}_{20}(\text{OH})_4]$  (Lee and Guggenheim 1981). A cluster of two complete octahedra was selected  $\{[\text{Al}_2\text{O}_8(\text{OH})_2]^{12-}\}$  in an edge-sharing disposition, where the hydroxylic O atoms are bridging both octahedra as in the montmorillonite structure. This cluster was neutralized saturating the dangling bonds re-

sulting from the homolytic cut with hydrogens. Then, four terminal OH groups are formed in the same plane (M-OH-M') and four terminal  $\text{OH}_2$  groups are formed in the rest of the octahedral co-ordination positions. Thus, the cluster model generated has the formula  $\text{Al}_2(\text{OH})_2(\text{OH})_4(\text{OH}_2)_4$ . Different isomorphous substitutions of  $\text{Al}^{3+}$  by  $\text{Fe}^{3+}$  and  $\text{Mg}^{2+}$  were realized in this cluster, generating the following based cation pair clusters (Fig. 1):  $\text{AlAl} \equiv [\text{Al}_2(\text{OH})_2(\text{OH})_4(\text{OH}_2)_4]$ ,  $\text{AlFe} \equiv [\text{AlFe}(\text{OH})_2(\text{OH})_4(\text{OH}_2)_4]$ ,  $\text{AlMg} \equiv [(\text{AlMg}(\text{OH})_2(\text{OH})_4(\text{OH}_2)_4)^-]$ ,  $\text{AlMgH} \equiv [\text{AlMg}(\text{OH})_2(\text{OH})_3(\text{OH}_2)_5]$ ,  $\text{FeFe} \equiv [\text{Fe}_2(\text{OH})_2(\text{OH})_4(\text{OH}_2)_4]$ ,  $\text{FeMg} \equiv [(\text{FeMg}(\text{OH})_2(\text{OH})_4(\text{OH}_2)_4)^-]$ ,  $\text{MgMg} \equiv [(\text{Mg}_2(\text{OH})_2(\text{OH})_4(\text{OH}_2)_4)^{2-}]$ , and  $\text{MgMgH}_2 \equiv [\text{Mg}_2(\text{OH})_2(\text{OH})_3(\text{OH}_2)_6]$ .

For the *ab initio* calculations, the Hartree-Fock (HF) approximation was used in the GAUSSIAN-94 program (Frisch et al. 1995; Hehre et al. 1986). All clusters were calculated with the restricted Hartree-Fock (RHF) approximation except the AlFe and FeMg, which were calculated by unrestricted Hartree-Fock (UHF) approach because of their odd electron number. Taking into account that the  $\text{Fe}^{3+}$  in octahedral co-ordination can be in its low spin configuration (Liebau 1985), FeX (X = Al and Mg) and FeFe clusters were considered as doublet and singlet spin multiplicities, respectively. These molecular cluster structures were determined by searching the molecular potential energy surface (PES) for critical points with respect to all atomic coordinates. We employed standard double- $\zeta$  basis set with polarization functions augmented by diffuse functions (6-31+G\*) (Foresman and Frisch 1993). Diffuse functions (+) allow orbitals to occupy a larger region of space to describe better systems where electrons are relatively far from the nucleus. By means of these diffuse functions, we try to describe anionic and lone pair structures that are present in our clusters. Our preliminary calculations without diffuse functions confirmed that diffuse functions are helpful in obtaining the critical points of the PES with a geometry that is reasonably comparable to the experimental one. In addition, Dunning-Huzinaga full double zeta basis set (D95) including pseudopotentials (LANL2DZ) was also used. The geometries of all clusters were fully optimized in the same basis set in each case by the Berny method (Schlegel 1982). Vibrational modes and frequencies were obtained from the force constant analysis and the frequencies were scaled by the standard factor 0.89 to account for anharmonic effects, the neglect of electron correlation, and limitations of the basis set (Pople et al. 1981; Gordon and Truhlar 1986), before comparison with experimental values. This systematic scaling for the calculated vibrational frequencies is very often used in the most *ab initio* studies and they are well established in quantum chemistry (Lasaga 1992; Sauer et al. 1994; Hehre et al. 1986) and in many *ab initio* molecular cluster studies on minerals (Kubicki and Apitz 1998; Kubicki et al. 1996, 1997, 1999).

## RESULTS AND DISCUSSION

### Geometry and electronic structure

Figure 1 shows optimized structures of the edge-sharing dioctahedral clusters. The general geometry of these clusters is close to the disposition of the octahedra in the octahedral layer

of clays. In the AlAl cluster, different positions of the OH<sub>2</sub> groups were tested maintaining the dioctahedral structure, such as, those either with the OH<sub>2</sub> groups in the Al-O-Al plane (Kubicki and Apitz 1998) or with these groups in perpendicular planes with respect to the Al-O-Al plane. However, the clusters with the O atoms of OH<sub>2</sub> groups in a perpendicular disposition with respect to the M-OH-M' plane (Fig. 1) were the best configurations for our samples and working conditions. Within the Al(OH)Al(OH) ring, the experimental OAlO and AlOAl angles in gibbsite are approximately 80 and 100°, respectively (Saalfeld and Wedde 1974), compared with the 74.5° and 105.5° obtained in our calculations, respectively. Similar values were found in the other clusters in the range of 68–80° and 103–106° for OMO and MOM' angles, respectively. The bridging OH hydrogens are in the same plane of M-OH-M'-OH-M ring (Fig. 1).

The main geometrical features of these clusters calculated at different levels are presented in Table 1. In general, good similarities were found between the theoretically calculated M-M', M-O(H), and O-H (M-OH-M') bond lengths and the experimental values. In the most cases, the geometrical parameters, calculated at 6-31+G\* level, are slightly closer to experimental data than those calculated at LANL2DZ level. In the M-M' interatomic distance, our cluster model reproduces the experimental values in most of the cases. For example, in pyrophyllite, the experimental Al...Al distance is 2.97 Å (XRD data from Lee and Guggenheim 1981) and the value calculated at 6-31+G\* level is 2.98 Å for the AlAl cluster. The Al-Mg distance found in our cluster are identical (3.05 Å) to the experimental values from the AlMg cation pairs of the octahedral sheet of hydroxalclites (Cavani et al. 1991). Also identical Mg-Mg distances (3.15 Å) are found between the theoretical value of the cluster and the experimental value from brucite (Catti et al. 1995). The M...M' distance increases with the substitution of Al by Mg (AlAl < AlMg < MgMg) as it was expected from the higher ionic radius of Mg<sup>2+</sup> than Al<sup>3+</sup>. However, in the FeFe cluster the d(M-M') distance is smaller than in the other clusters. The protonation of the MgMg to form MgMgH<sub>2</sub> produces a shortening of the M...M' distance. This fact can be explained by a decrease of the repulsion interactions between the O atoms, which have less negative charge in MgMgH<sub>2</sub> than in MgMg. Concerning the M-OH bond length for the bridging OH groups, in general, the theoretical calculations of the cluster models reproduce the experimental values. In the AlAl cluster

our value is 1.89 Å, whereas the experimental values in pyrophyllite (Lee and Guggenheim 1981) and gibbsite (Saalfeld and Wedde 1974) are 1.89 and 1.88–1.92 Å, respectively. In the FeFe cluster, the calculated Fe-O bond length is shorter than the experimental value, although our theoretical value is identical (1.88 Å) to that obtained previously from periodic ab initio methods in hematite (Becker et al. 1996). It is remarkable that only small differences in the O-H bond length (M-OH-M') are observed with the isomorphous substitution. The calculated values for AlAl (0.94 Å) and MgMg (0.946 Å) clusters are similar to the experimental values obtained for mica (0.947 Å, Catti et al. 1994) and brucite (0.958 Å, Catti et al. 1995), respectively. Our calculated O-H bond length is consis-

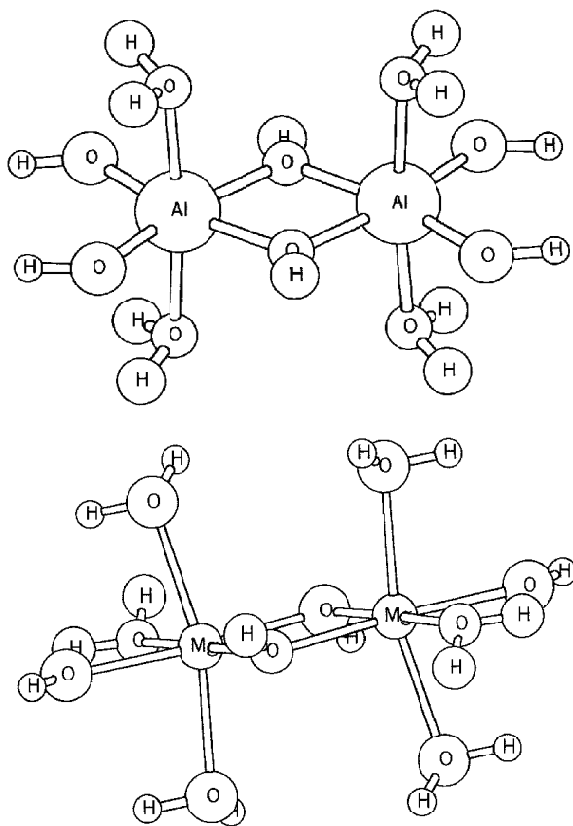


FIGURE 1. Optimized geometries of the edge-sharing dioctahedral clusters: AlAl (a) and MgMgH<sub>2</sub> (b).

TABLE 1. Main geometrical features of the molecular clusters

Cluster (MM')	d (M-M')		d [M-O(H) (M-OH-M')]		d [O-H (M-OH-M')]	
	Calc.*	expt.	Calc.*	expt.†	Calc.*	expt.
AlAl	3.00 (2.98)	2.97‡	1.89 (1.87)	1.89‡ (1.88–1.92)	0.944 (0.944)	0.947§ 0.94
AlFe	3.02		1.95, 1.85		1.94	
AlMg	3.06 (3.05)	3.05#	1.88, 2.01 (1.82, 2.04)	1.89‡, 2.03	0.945 (0.942)	
AlMgH	(3.05)	3.05#	(1.88, 1.99)		(0.944)	
FeFe	2.94		1.88	2.00	0.951	
FeMg	3.19	3.11†	1.88, 2.17	2.06	0.946	
MgMg	3.09 (3.15)	3.15**	1.97 (1.99)	2.06	0.9455 (0.942)	0.958**
MgMgH <sub>2</sub>	(3.03)		(2.02)	2.06	(0.944)	

\* From calculations at LANL2DZ level, values in brackets are from calculations at 6-31+G\* level.

† From Wederpohl 1978 (values in brackets for gibbsite: Saalfeld and Wedde 1974).

‡ From Lee and Guggenheim (1981).

§ In muscovite (Catti et al. 1994).

|| In dickite (Bish and Johnston 1993).

# Cavani et al. 1991.

\*\* In brucite (Catti et al. 1995).

tent with that obtained previously by periodic ab initio quantum mechanical methods in brucite (0.95 Å, Sherman 1991).

To study the electronic structure of these clusters, a Mulliken population analysis was performed (Table 2). It is well known that the atomic charge is not a quantum mechanical observable; hence, any method for computing it will be arbitrary. However, though Mulliken population analysis calculates charges by dividing overlap population evenly between the two atoms involved in each bond and it depends on the basis set, this approximation can be useful for calculating relative differences within a certain basis set in a series of clusters. Some differences can be observed among the calculated clusters. In the clusters with  $\text{Fe}^{3+}$  the charge on each Fe atom is lower than on other cations. No significant difference is detected in the atomic charges of the bridging OH atoms for the Al and Mg clusters, however this value is lower in the FeFe cluster. This fact can probably be due to the high covalent character of the Fe-O bond (Sherman 1985). Concerning the hydrogen atom of the M-OH-M' groups, the positive charge on the hydrogen decreases with the increasing substitution of Al by Mg in all basis sets studied, according with the increasing order of basicity of these clusters (Cavani et al. 1991). The same effect is observed with the substitution of Fe by Mg.

### Vibrations of OH groups

Our initial hypothesis is that the effect of the crystal lattice structure on the bridging OH vibrational properties is constant in our series and the influence of the cation substitution in the octahedral sheet on the bridging OH vibration frequencies depends on the local environment structure. This effect will depend mainly on the nature of the cations that are joined directly to these OH groups and are exchanged in the isomorphous substitution. Therefore, theoretical molecular models described above can be used to represent microscopically one part of minerals where octahedral layers are present. The frequencies and relative intensities of the stretching and bending vibrations of the bridging OH groups in the clusters studied are presented in Table 3 along with experimental data.

In these clusters, three types of OH groups can be distinguished taking into account the normal modes analysis on these OH vibrations: bridging OH, terminal OH and terminal  $\text{OH}_2$ . Because the terminal OH and  $\text{OH}_2$  groups do not exist in the clay crystal lattice and they are a consequence of the model, we concentrated on the bridging OH groups. Observing the contributions of the vibrational movements of all atoms of each cluster to the normal vibration modes of the bridging OH groups, only the bridging OH hydrogen displacements contrib-

ute to these modes in all clusters. This means that each of the bending,  $\delta(\text{OH})$  (in-plane) and  $\gamma(\text{OH})$  (out-of-plane), and stretching,  $\nu(\text{OH})$ , vibrational modes for these OH groups are completely separated from the others, and each one of these uncoupled modes appears at different frequencies as in the spectroscopic data.

With respect to the  $\nu(\text{OH})$  bands of the bridging OH (M-OH-M') groups, a linear correlation ( $R = 0.9883$ ) between the O-H bond lengths and  $\nu(\text{OH})$  frequencies was found for all MM' clusters (Fig. 2). This is consistent with other cluster models of aluminum oxides and aluminum oxyhydroxide (Kubicki and Apitz 1998). In clays, the  $\nu(\text{OH})$  bands appear at lower frequencies than those calculated in all M-OH-M' cases. This fact can be explained by the existence of hydrogen bond in the clay structure between the hydrogen of this bridging OH group and the apical O atoms of the tetrahedral sheet (Robert and Kodama 1988), which are not included in our clusters. In minerals, where the involvement of this bridging OH group in a hydrogen bond is lower (e.g., gibbsite), the  $\nu(\text{OH})$  frequency calculated ( $3739 \text{ cm}^{-1}$ , for the AlAl cluster) matches well with the experimental value of gibbsite ( $3740\text{--}3745 \text{ cm}^{-1}$ , Table 3; Boehm and Knözinger 1983).

It is remarkable that this hydrogen bond affects mainly the stretching vibrations, whereas the bending frequencies do not change significantly with this hydrogen bond. The substitution of Si by Al in the tetrahedral sheet of clays produces an increase of the hydrogen bond strength between the apical O atoms of this tetrahedral sheet and the M-OH-M' group of the octahedral sheet, due to the increasing negative charge on these O atoms of the tetrahedral layer. This effect produces a decrease of the  $\nu(\text{OH})$  frequency of this OH (M-OH-M') group. Sometimes, when the interlayer cation is very close to these apical O atoms, as in the case of potassium, this effect is partially neutralized. Then, we should consider at least two different domains around the M-OH-M' group for comparative studies: (1) a pyrophyllite or smectite domain where the substitution of Si by Al is low; and (2) a mica or illite domain, where the substitution of Si by Al is higher and the hydrogen bond effect on the octahedral M-OH-M' group will be stronger than in the former domain. Considering the same chemical composition in the tetrahedral layer and interlayer space for all species studied, the effect of the hydrogen bonds, coming from

**TABLE 2.** Mulliken net atomic charges of the calculated clusters (at LANL2DZ level)

Cluster	M, M'	O (M-OH-M')	H (M-OH-M')
AlAl	1.916	-1.154	0.46
AlFe	1.978 (Al) 1.291 (Fe)	-1.05	0.48
AlMg	1.927 (Al) 1.233 (Mg)	-1.16	0.426
FeFe	1.203	-0.828	0.474
FeMg	1.231 (Fe) 1.424 (Mg)	-1.00	0.417
MgMg	1.308	-1.134	0.396

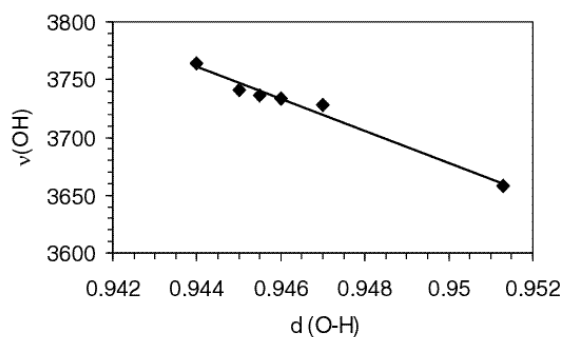


**FIGURE 2.** Plot of O-H bond lengths (in angstroms) vs.  $\nu(\text{OH})$  frequencies (in  $\text{cm}^{-1}$ ) calculated at LANL2DZ level of the M-OH-M' groups.

**TABLE 3.** Calculated and experimental vibration frequencies of the bridging OH groups (M-OH-M')

Cluster	$\delta$ (OH)			$\gamma$ (OH)		$\nu$ (OH)		
	LanL2DZ	(6-31+G*)	expt.*	LanL2DZ	(6-31+G*)	LanL2DZ	(6-31+G*)	expt.
AlAl	915 (1113)	914 (811)	915 914†	664	449	3764 (253)	3739 (234)	3740-3745‡ 3675\$, 3641-3621
AlFe	903 (931)		875 890#	660		3739 (151), 3718 (295)		3652\$ 3573
AlMg	851(157), 823(642)	841 (334) 796 (57) 834 (406)	845 820, 796**	611	424	3738 (13), 3744 (55)	3755 (123)	3682\$ 3604
AlMgH							3720 (82)	
FeFe	774 (56)		797	381		3658 (833)		3631\$, 3535
FeMg	716 (57)		780	441		3734 (67), 3733 (41)		3571††
MgMg	706 (613)	685 (428)	669†	597	492	3736 (16)	3752 (51)	3583
MgMgH <sub>2</sub>		678 (374)					3714 (21)	3700†, **

Note: Frequencies in cm<sup>-1</sup>, intensity values in brackets.

\* In smectite/illite (Cuadros and Altaner 1998).

† Farmer 1974.

‡ In gibbsite (Saalfeld and Wedde 1974).

\$ Pyrophyllite domain in dioctahedral mica (Besson and Drits 1997).

|| Mica domain in dioctahedral mica (Besson and Drits 1997).

# In montmorillonite (Bishop et al. 1994).

\*\* Van der Marel and Beutelspacher 1976.

†† Madejová et al 1994.

the tetrahedral sheet, on the OH vibrations can be considered constant for all M-OH-M' species studied in this work. A linear correlation is found between the values calculated and the experimental data from dioctahedral micas ( $R = 0.9216$ , Fig. 3). A similar linear relationship is found with experimental values of smectites, but with a worse correlation, because of the high dispersion of experimental data from different authors, due to the high variability in the tetrahedral charge and interlayer cation composition of the natural samples.

The relative variation of calculated  $\nu$ (OH) frequencies with the isomorphous substitution of octahedral cations is similar to the experimental behavior in all cases. Previous papers (Vedder 1964; Robert and Kodama 1988; Besson and Drits 1997) have reported that this cation substitution effect can be related with the change of the mass sum and the valence sum of both cations joined to the bridging OH group. The  $\nu$ (OH) depends on the OH bond strength,  $K_{OH}$ , and the reduced mass of the vibration system,  $\mu_{OH}$ :

$$\nu_{OH} = \frac{1}{2\pi c} \sqrt{\frac{K_{OH}}{\mu_{OH}}} \quad (1)$$

To justify our correlation of  $\nu$ (OH) frequency vs. cationic mass sum, it can be assumed that the OH vibration also depends on the mass of cations associated with the OH groups. Previous experimental studies about the cation substitution effect on the  $\nu$ (OH) frequency reported the effect of these parameters separately in triads where the variation of one parameter is more important than the another one (i.e., AlFe series (AlAl, AlFe, and FeFe) for mass increasing, or AlMg series (AlAl, AlMg, and MgMg) for valence variation) for a better understanding of these effects (Vedder 1964; Robert and Kodama 1988; Besson and Drits 1997). Following this methodology in the AlFe and FeMg triad series, semi-quantitative trends are found between the  $\nu$ (OH) frequency and the atomic weight sum of both M, M' cations (Fig. 4a). The tendency found in the theoretical frequencies is similar to that observed in experimental values. The  $\nu$ (OH) frequency decreases as the mass of these cations increases. This effect was also found experimentally in brucite-like divalent metal hydroxides (Brindley and Kao 1984) and in dioctahedral micas (Besson and Drits 1997).

Following Vedder's model (1964), the  $K_{OH}$  value depends on the valence of cations bonded to OH groups, because the OH bond will be stronger by the decreasing of this common charge for both atoms (Besson and Drits 1997). Accordingly, the  $\nu$ (OH) frequency should decrease with an increasing in the sum of valences of the corresponding cation pairs. However, Robert and Kodama (1988) found the opposite effect. Besson and Drits (1997) found in dioctahedral micas that the Vedder model only applies sometimes. Triads of combinations of cations with similar atomic weight present the opposite relationship [ $\nu$ (OH) / valence sum for MM' in M-OH-M' group] that the corresponding to Vedder model. We found a similar relationship in our theoretical calculations, an increasing of the  $\nu$ (OH) frequency with the increasing of the sum of cation pair valences for the AlMg triad (MgMg, MgAl, and AlAl). However, the relationship proposed by Vedder (1964) [decreasing of  $\nu$ (OH) frequency with an increasing of valence sum] seems to be valid for combinations of cations of the FeMg series (MgMg, MgFe, and FeFe). In this series, a similar relationship was found in experimental  $\nu$ (OH) values and in our calculated values. The Vedder model takes the classical concept of the valence in the cations corresponding to ionic solids. However, in these minerals, the bonds are not completely ionic, they are polarized covalent bonds. The valence concept in the substitution cations does not describe sufficiently the variation of the

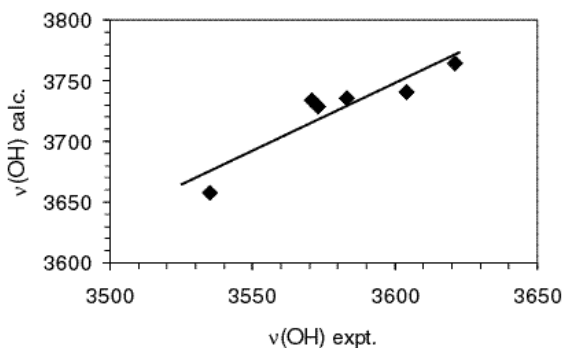


**FIGURE 3.** Correlation between the calculated values (at LANL2DZ level) and experimental data of the  $\nu$ (OH) frequency (in cm<sup>-1</sup>) of bridging OH groups for a mica environment (Besson and Drits 1997; Madejová et al. 1994).

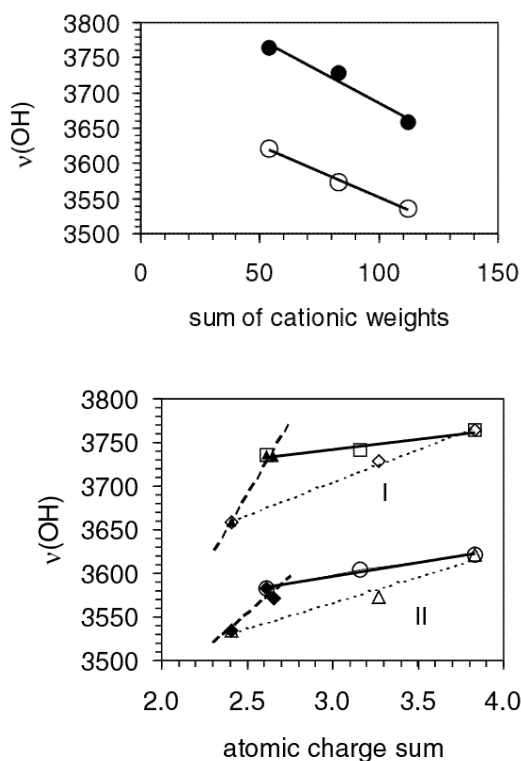


**FIGURE 4.** Cation substitution effect on the experimental and calculated (at LANL2DZ level)  $\nu(\text{OH})$  frequencies (in  $\text{cm}^{-1}$ ) of the bridging OH groups. Relationship with (a) atomic weights (AlAl, AlFe, and FeFe series, hollow circles are experimental frequencies), and (b) Mulliken atomic charges of cations bonded to these OH groups (I and II mean theoretical and experimental values, respectively; full, dashed and dotted lines correspond to the AlMg, FeMg, and AlFe series, respectively).

atomic charge in a series of cluster. However, the Mulliken population analysis would show us a more suitable description of the atomic charge variation in our series, according with the wave-function of our calculations. Hence, the Mulliken atomic charge could be a better magnitude than the valence for describing the variation of the OH vibrational frequency with respect to the isomorphic substitution effect. An increase in theoretical  $\nu(\text{OH})$  frequency with the sum of these atomic charges was observed in all cases (Fig. 4b), without finding any contradiction in the slope between different MM' series. Similar relationships were found using experimental values of  $\nu(\text{OH})$  frequencies (Fig. 4b).

Hence, at least two factors, the mass sum and Mulliken atomic charge sum of the cations bonded to the bridging OH group affect to the  $\nu(\text{OH})$  frequency shift. Fitting the experimental  $\nu(\text{OH})$  frequency of dioctahedral micas directly and simultaneously to both factors by means of a multiple regression analysis gives:

$$\nu(\text{OH}) = 3508 (\pm 39.8) - 0.725 (\pm 0.21) m + 42.5 (\pm 9.9) q \quad (2)$$

$$(R^2 = 0.9511)$$

where  $m$  is the cation pair mass sum and  $q$  is the Mulliken atomic charge sum of the cations bonded to this bridging OH group. This correlation provides a better fit than taking into account  $m$  and the valence sum. The intercept term of the Equation 2 could be considered as the OH vibration frequency of the isolated OH group without the influence of the mass and charge cations. Experimental  $\nu(\text{OH})$  values corresponding to a smectite domain yield a similar relationship but with worse correlation coefficient, since it is difficult to find experimental data for all M-OH-M' species with the same low tetrahedral charge and M-OH-M' environment from natural samples.

In all these relationships, similar tendencies were found from mineral crystal lattice experimental data and theoretical calculations from small dioctahedral clusters. This fact could mean that the weak hydrogen bonds between the OH group and the apical O atoms of the tetrahedral sheet will decrease the  $\nu(\text{OH})$  frequency proportionally in all M-OH-M' species, and the relative relationships will remain constant. This means that the effect of the tetrahedral sheet and interlayer cations on the influence of cation substitution in the octahedral sheet on the OH vibration frequency can be considered constant in our systems.

A good agreement is found between the bridging OH  $\delta(\text{OH})$  frequencies (in-plane bending vibration) calculated for these clusters and the experimental  $\delta(\text{OH})$  values of the M-OH-M' groups in clays (Table 3). A linear relationship is found between the experimental data and the values from our calculations ( $R = 0.9704$ , Fig. 5). This fact means that the possible hydrogen bonds between the bridging OH hydrogens and the apical O atoms of the tetrahedral sheet do not affect significantly the  $\delta(\text{OH})$  frequencies. The  $\gamma(\text{OH})$  bands (out of plane bending vibration) have not been assigned experimentally in many minerals, since they appear in the same region of the M-O-M' vibrations and structural vibrations of these solids and it is difficult to distinguish them. Our calculated values of  $\gamma(\text{OH})$  frequencies can be a good estimation and help for interpreting these bands, taking into account the above good agreement among the experimental and calculated  $\delta(\text{OH})$  frequencies.

The cation substitution effect on the  $\delta(\text{OH})$  and  $\gamma(\text{OH})$  frequencies of the bridging OH groups (M-OH-M') is also observed. In general, considering all clusters together, an increase in the calculated  $\delta(\text{OH})$  and  $\gamma(\text{OH})$  frequencies is observed with the Mulliken atomic net charge sum of the cation pairs (Fig. 6) as in  $\nu(\text{OH})$ . Similar behavior was found for the experimental  $\delta(\text{OH})$  frequencies. Taking into account the different MM' triad series, similar linear relationships were found like in  $\nu(\text{OH})$ . With respect to the cation mass effect, the  $\delta(\text{OH})$  and  $\gamma(\text{OH})$  frequencies decreases with the increasing of the mass of cation pair in the AlFe series (FeFe, FeAl, AlAl), like in  $\nu(\text{OH})$ . On the contrary, the behavior in FeMg (FeFe, FeMg, MgMg) and AlMg (AlAl, AlMg, MgMg) series is the opposite, an increasing of  $\delta(\text{OH})$  frequency with the mass of cations. Possibly the cation charge effect could be higher in the  $\delta(\text{OH})$  vibration than in  $\nu(\text{OH})$  for these systems. The  $\delta(\text{OH})$  experimental data have similar behavior to our calculations. The behavior of the  $\gamma(\text{OH})$  vibration is similar to  $\delta(\text{OH})$  in all cases, except in the FeMg triad series where the tendency is contrary to  $\delta(\text{OH})$ . Probably the cation mass effect is more important in  $\gamma(\text{OH})$  frequency

shift than in  $\delta(\text{OH})$ , like in  $\nu(\text{OH})$ . With these results, we try to correlate the experimental  $\delta(\text{OH})$ , theoretical  $\delta(\text{OH})$ , and calculated  $\gamma(\text{OH})$  frequency shifts directly and simultaneously with both parameters, masses sum and the sum of Mulliken atomic charge of cations, by means of multiple regression analysis. A similar correlation equation for all these frequencies was obtained [Eq. 3 for theoretical  $\delta(\text{OH})$ , Eq. 4 for experimental  $\delta(\text{OH})$ , and Eq. 5 for theoretical  $\gamma(\text{OH})$  values]:

$$\delta(\text{OH}) = 2.195 (\pm 0.451)m + 216.804 (\pm 11.155)q \quad (3)$$

$$(R^2 = 0.9989)$$

$$\delta(\text{OH}) = 2.741 (\pm 0.280)m + 205.812 (\pm 6.931)q \quad (4)$$

$$(R^2 = 0.9996)$$

$$\gamma(\text{OH}) = -0.838 (\pm 0.989)m + 205.803 (\pm 24.478)q \quad (5)$$

$$(R^2 = 0.9891)$$

The agreement with experimental data in  $\delta(\text{OH})$  tell us that

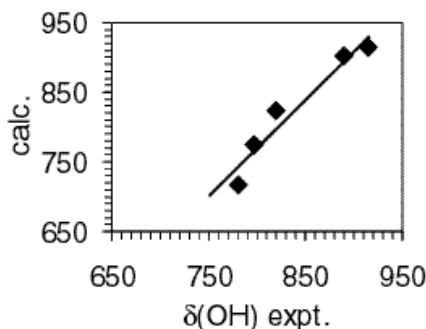


FIGURE 5. Bending vibration frequencies  $\delta(\text{OH})$  (in  $\text{cm}^{-1}$ ) of bridging OH groups. Experimental data (Table 3) vs. values calculated theoretically at LANL2DZ level.

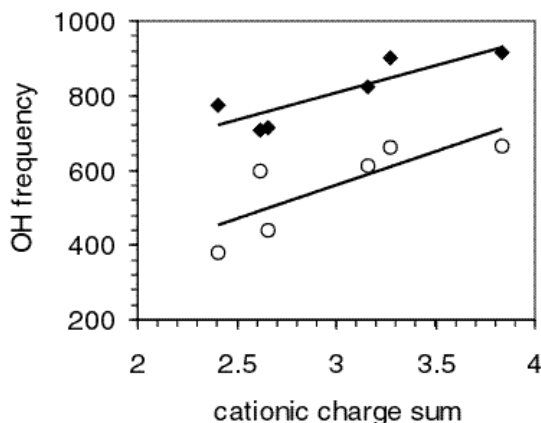


FIGURE 6. Cation substitution effect on the theoretical (at LANL2DZ level)  $\delta(\text{OH})$  and  $\gamma(\text{OH})$  frequencies (in  $\text{cm}^{-1}$ ) of the bridging OH groups for all clusters. Relationship with the sum of the Mulliken atomic net charge of the cations bonded to OH groups [hollow circles correspond to  $\gamma(\text{OH})$ ].

this theoretical approach can be useful for the  $\gamma(\text{OH})$  bands assignment. Notice that these equations do not present an intercept term, because the free OH groups cannot yield the  $\delta(\text{OH})$  and  $\gamma(\text{OH})$  frequencies.

## CONCLUSIONS

The calculated values of the  $\nu(\text{OH})$  frequencies reproduce the experimental values of gibbsite, but not those of clays. In clays, the O-H bond of the bridging OH group is oriented toward the apical O atoms of the tetrahedral sheet and forms weak hydrogen bond interactions with these apical O atoms, which decrease the  $\nu(\text{OH})$  frequency. This hydrogen bonds are not included in our model. However, the calculated frequencies in our models present a relative behavior with respect to the isomorphous substitution of octahedral sheet cations similar to the experimental data. This fact means that the effect of the tetrahedral sheet and interlayer cations on the influence of these octahedral cation substitutions on the OH vibrations is constant. Our theoretical studies are useful to clear up the present discrepancies about the correlation between the  $\nu(\text{OH})$  frequencies and the nature of the cations joined to these OH groups. Because the bonds in silicates are not completely ionic and have a certain grade of covalent character, the net electronic charge of each cation can be a useful parameter to analyze the isomorphous cation substitution effect on the OH vibration frequencies. This electronic net charge can be determined by means of the Mulliken approximation in our quantum mechanical approach. Good correlations were found between the Mulliken atomic charges and atomic weights of cations, and the theoretical and experimental OH frequencies. The same trends and slopes are found for theoretical and experimental behavior of the cation substitution effect on the OH vibration frequencies.

Comparing our theoretical results with spectroscopic data from clays, the  $\nu(\text{OH})$  vibration seems to be sensitive to the hydrogen bonds with the apical O atoms of the tetrahedral sheet. Since this interaction changes with the Al composition in the tetrahedral sheet, the  $\nu(\text{OH})$  frequency will also depend on the tetrahedral Al content. This fact could affect the spectroscopic studies on cation distribution in the octahedral sheet of smectite-illite systems where different tetrahedral environments can produce broadening or fine structures in the IR bands. On the contrary, our results show that the  $\delta(\text{OH})$  frequencies will not depend significantly on these hydrogen bond interactions. Therefore, we suggest considering the  $\delta(\text{OH})$  bands as an indicator in further cation distribution studies of smectite-illite systems.

## ACKNOWLEDGMENTS

This work was supported by the DGES grant PB97-1205. Authors are grateful to J. Kubicki and J. Cuadros by their fruitful comments and discussions and to the "Centro de Cálculo de la Universidad de Granada," "Centro de Cálculo del CIEMAT-Madrid," and "Centro de Computación de Galicia" for allowing the use of their computational facilities.

## REFERENCES CITED

- Becker, U., Hochella, M.F. Jr., and Apra, E. (1996) The electronic structure of hematite (001) surfaces: applications to the interpretation of STM images and heterogeneous surface reactions. *American Mineralogist*, 81, 1301-1314.
- Besson, G. and Drits, V.A. (1997) Refined relationship between chemical composition of dioctahedral fine-grained micaceous minerals and their infrared spectra

- within the OH stretching region. Part II: The main factors affecting OH vibrations and quantitative analysis. *Clays and Clay Minerals*, 45, 170–183.
- Bish, D.L. and Johnston, C.T. (1993) Rietveld refinement and fourier-transform infrared spectroscopic study of the dickite structure at low temperature. *Clays and Clay Minerals*, 41, 297–304.
- Bishop, J.L., Pieters, C.M., and Edwards, J.O. (1994) Infrared spectroscopic analyses on the nature of water in montmorillonite. *Clays and Clay Minerals*, 42, 702–716.
- Bleam, W.F. (1993) Atomic theories of phyllosilicates: quantum chemistry, statistical mechanics, electrostatic theory, and crystal chemistry. *Reviews of Geophysics*, 31, 51–73.
- Boehm, H.P. and Knözinger, H. (1983) Nature and estimation of functional groups on solid surfaces. In J.R. Anderson and M. Bouchart, Eds., *Catalysis Science and Technology*, pp. 39–207. Springer, New York.
- Bridgeman, C.H., Buckingham, A.D., Skipper, N.T., and Payne, M.C. (1996) Ab initio total energy study of uncharged 2:1 clays and their interaction with water. *Molecular Physics*, 89, 879–888.
- Brindley, G.W. and Kao, C.C. (1984) Structural and IR relations among brucite-like divalent metal hydroxides. *Physics and Chemistry of Minerals*, 10, 187–191.
- Catti, M., Ferraris, G., Hull, S., and Pavese, A. (1994) Powder neutron diffraction study of 2M1 muscovite at room pressure and at 2 GPa. *European Journal of Mineralogy*, 6, 171–178.
- (1995) Static compression and H disorder in brucite,  $\text{Mg}(\text{OH})_2$ , to 11 GPa: a powder neutron diffraction study. *Physics and Chemistry of Minerals*, 22, 200–206.
- Cavani, F., Trifiro, F. and Vaccari, A. (1991) Hydrotalcite-type anionic clays: preparation, properties and application. *Catalysis Today*, 11, 173–301.
- Collins, D.R. and Catlow, C.R. (1992) Computer simulations of structures and cohesive properties of micas. *American Mineralogist*, 77, 1172–1181.
- Cuadros, J. and Altaner, J. (1998) Compositional and structural features of the octahedral sheet in mixed layer illite/smectite from bentonites. *European Journal of Mineralogy*, 10, 111–124.
- Cuadros, J., Sainz-Diaz, C.I., Ramirez, R., and Hernandez-Laguna, A. (1999) Analysis of Fe segregation in the octahedral sheet of bentonitic illite/smectite by means of FT-IR,  $^{27}\text{Al}$  MAS NMR and inverse Monte Carlo simulations. *American Journal of Science*, 299, 289–308.
- Farmer, V.C. (1974) The layer silicates. In V.C. Farmer, Ed., *The infrared spectra of minerals*, p. 331–363. Mineralogical Society, London.
- Foresman, J.B. and Frisch, A.E. (1993) Exploring chemistry with electronic structure methods. Gaussian, Inc., Pittsburgh, Pennsylvania.
- Frisch, M. J., Trucks, G.W., Schlegel, H.B., Gill, P.M.W., Johnson, B.G., Robb, M.A., Chessemann, J. R., Keith, T.A., Petersson, G.A., Montgomery, J.A., Raghavachari, K., Al-Laham, M.A., Zarzewski, V.G., Ortiz, J.V., Foresman, J.B., Cioslowski, J., Stefanov, B.B., Nanayakkara, A., Challacombe, M., Peng, C.Y., Ayala, P.Y., Chen, W., Wong, M.W., Andres, J.L., Replogle, E.S., Gomperts, R., Martin, R.L., Fox, D.J., Binkley, J.S., Defrees, D.J., Baker, J., Stewart, J.J.P., Head-Gordon, M., Gonzalez, C., and Pople, J.A. (1995) Gaussian 94 Revision A.1. Gaussian Inc., Pittsburgh, Pennsylvania.
- Giese, R.F. (1979) Hydroxyl orientations in 2:1 phyllosilicates. *Clays Clay Minerals*, 27, 213–223.
- Gordon, M.S. and Truhlar, D.G. (1986) Scaling all correlation energy in perturbation theory calculations of bond energies and barrier heights. *Journal of American Chemical Society*, 108, 5412–5419.
- Güven, N. (1988) Smectites. In *Mineralogical Society of America Reviews in Mineralogy*, 19.
- Hehre, W.J., Radom, L., Schleyer, P.R. and Pople, J.A. (1986) *Ab initio molecular orbital theory*, 548 p. Wiley Interscience, New York.
- Hobbs, J.D., Cygan, R.T., Nagy, K.L., Schultz, J., and Sears, M.P. (1997) All-atom ab initio energy minimization of the kaolinite crystal structure. *American Mineralogist* 82, 657–662.
- Karaborni, S., Smit, B., Heidug, W., Urai, J., and Van Oort, E. (1996) The swelling of clays: Molecular simulations of the hydration of montmorillonite. *Science*, 271, 1102–1104.
- Kubicki, J.D. and Apitz, S.E. (1998) Molecular cluster models of aluminum oxide and aluminum hydroxide surfaces. *American Mineralogist*, 83, 1054–1066.
- Kubicki, J.D., Blake, G.A., and Apitz, S.E. (1996) Ab initio calculations on aluminosilicate  $\text{Q}^3$  species: Implications for atomic structures of mineral surfaces and dissolution mechanisms of feldspars. *American Mineralogist*, 81, 789–799.
- (1997) Molecular orbital calculations for modeling acetate-aluminosilicate adsorption and dissolution reactions. *Geochimica et Cosmochimica Acta*, 61, 1031–1046.
- Kubicki, J.D., Sykes, D., and Apitz, S.E. (1999) Ab initio calculation of aqueous Aluminum and Aluminum-carboxylate complex energetics and  $^{27}\text{Al}$  NMR chemical shifts. *Journal of Physical Chemistry A* 103, 903–915.
- Lasaga, A.C. (1992) Ab initio methods in mineral surface reactions. *Reviews of Geophysics*, 30, 269–303.
- (1995) Fundamental approaches in describing mineral dissolution and precipitation rates. In *Mineralogical Society of America Reviews in Mineralogy* 31, 23–86.
- Lee, J.H. and Guggenheim, S. (1981) Single crystal X-ray refinement of pyrophyllite-17c. *American Mineralogist*, 66, 350–357.
- Liebau, F. (1985) *Structural Chemistry of Silicates*, 347 p. Springer-Verlag, Berlin.
- Madejová, J., Komadel, P., and Cícel, B. (1994) Infrared study of octahedral site populations in smectites. *Clay Minerals*, 29, 319–326.
- Orlando, R., Dovesi, R., Roetti, C., and Saunders, V.R. (1994) Convergence properties of the cluster model in the study of local perturbations in ionic systems. The case of bulk defects in MgO. *Chemical Physics Letters*, 228, 225–232.
- Payne, M.C., Teter, M.P., Allan, D.C., Arias, T.A., and Joannopoulos, J.D. (1992) Iterative minimization techniques for ab initio total-energy calculations: molecular dynamics and conjugate gradients. *Reviews of Modern Physics*, 64, 1045–1097.
- Pople, J.A., Schlegel, H.B., Krishnan, R., Defrees, D.J., Binkley, J.S., Frisch, M.J., Whiteside, R.A., Hout, R.F., and Hehre, W.J. (1981). Molecular-orbital studies of vibrational frequencies. *International Journal of Quantum Chemistry: Quantum Chemical Symposium*, 15, 269–278.
- Robert, J.L. and Kodama, H. (1988) Generalization of the correlation between hydroxyl-stretching wavenumbers and composition of micas in the system  $\text{K}_2\text{O}-\text{Mg}_2\text{O}-\text{Al}_2\text{O}_3-\text{SiO}_2-\text{H}_2\text{O}$ : A single model for trioctahedral and dioctahedral micas. *American Journal of Science*, 288A, 196–212.
- Saalfeld, H. and Wedde, M. (1974) Refinement of the crystal structure of gibbsite. *Zeitschrift für Kristallographie, Kristallgeometrie, Kristallphysik, Kristallchemie*, 139, 129–135.
- Sanchez-Portal, D., Ordejon, P., Artacho, E., and Soler, J.M. (1997) Density-functional method for very large systems with LCAO basis sets. *International Journal of Quantum Chemistry*, 65, 453–461.
- Sauer, J. (1989) Molecular models in ab initio studies of solids and surfaces: from ionic crystals and semiconductors to catalysts. *Chemical Reviews*, 89, 199–255.
- Sauer, J., Ugliengo, P., Garrone, E., and Saunders, V.R. (1994) Theoretical study of van der Waals complexes at surface sites in comparison with the experiment. *Chemical Reviews*, 94, 2095–2160.
- Schindler, P.W. and Stumm, W. (1987) The surface chemistry of oxides, hydroxides, and oxide minerals. In W. Stumm, Ed., *Aquatic Surface Chemistry: Chemical Processes at the mineral-water interface*, p. 83–110. Wiley Interscience, New York.
- Schlegel, H.B. (1982) Optimization of equilibrium geometries and transition structures. *Journal of Computational Chemistry*, 3, 214–218.
- Sherman, D.M. (1985) The electronic structures of  $\text{Fe}^{3+}$  co-ordination sites in iron oxides. Application to spectra, bonding and magnetism. *Physics and Chemistry of Minerals*, 12, 161–175.
- (1991) Hartree-Fock band structure, equation of state, and pressure-induced hydrogen bonding in brucite,  $\text{Mg}(\text{OH})_2$ . *American Mineralogist*, 76, 1769–1772.
- Smrcek, L. and Benco, L. (1996) Ab initio periodic Hartree-Fock study of lizardite 1T. *American Mineralogist*, 81, 1405–1412.
- Tossell, J.A. and Vaughan, D.J. (1992) *Theoretical geochemistry: Application of quantum mechanics in the earth and mineral sciences*, p. 514. Oxford University Press, New York.
- Van der Marel, H.W. and Beutelspacher, H. (1976) *Atlas of infrared spectroscopy of clay minerals and their admixtures*. Elsevier, Amsterdam.
- Vedder, W. (1964) Correlations between infrared spectrum and chemical composition of mica. *American Mineralogist*, 49, 736–768.
- Wederpohl, K.H. (1978) *Handbook of Geochemistry*, Springer-Verlag.
- Winkler, B., Milman, V., and Payne, M.C. (1994) Orientation, location, and total energy of hydration of channel  $\text{H}_2\text{O}$  in cordierite investigated by ab initio total energy calculations. *American Mineralogist*, 79, 200–204.
- Winkler, B., Milman, V., Hennion, B., Payne, M.C., Lee, M.-H., and Lin, J.S. (1995) Ab initio total energy study of brucite, diasporite and hypothetical hydrous wadsleyite. *Physics and Chemistry of Minerals*, 22, 461–467.
- Xiao, Y. and Lasaga, A.C. (1994) Ab initio quantum mechanical studies of the kinetics and mechanisms of silicate dissolution:  $\text{H}^+$  ( $\text{H}_3\text{O}^+$ ) catalysis. *Geochimica et Cosmochimica Acta* 58, 5379–5400.